Published in final edited form as:

Pflugers Arch. 2022 April ; 474(4): 397–403. doi:10.1007/s00424-021-02653-9.

Neuronal allodynic mechanisms of Slc7a5 (LAT1) in the spared nerve injury rodent model of neuropathic pain

Aleyah E. Goins[1], **Kimberly Gomez**[2,3], **Dongzhi Ran**[2,3], **Mitra Afaghpour-Becklund**[1], **Rajesh Khanna**[2,3,4,†], **Sascha R.A. Alles**[1,†]

[1]Department of Anesthesiology and Critical Care Medicine, University of New Mexico School of Medicine, Albuquerque, NM 87106 United States of America

[2]Department of Pharmacology, College of Medicine, The University of Arizona, Tucson, Arizona, 85724, United States of America

[3]Comprehensive Pain and Addiction Center, The University of Arizona, Tucson, Arizona, 85724, United States of America

[4]Department of Molecular Pathobiology, College of Dentistry, New York University, 133 First Avenue Rm824, New York, NY 10010, USA

Abstract

High-impact chronic pain is suffered by 1 in 5 patients in the US and globally. Effective, non-addictive, non-opioid therapeutics are urgently needed for the treatment of chronic pain. Slc7a5 (Lat1), also known as system L-neutral amino acid transporter, is involved in a number of physiological processes related to inflammation. Transcriptomics studies have shown that Slc7a5 and its binding partner Slc3a2 are expressed in neurons of the dorsal root ganglia (DRG) and spinal dorsal horn, which are critical to the initiation and maintenance of nociception and pathophysiology of chronic pain. In addition, Slc7a5 is a transporter for the first-line anti-allodynic gabapentinoid drugs and binds to ion channels implicated in nociception and chronic pain including the voltage-gated sodium channel Nav1.7 and the voltage-gated potassium channels Kv1.1 and Kv1.2. We found that blocking Slc7a5 with intrathecal administration of the drug JPH203 alleviated allodynia in the spared nerve injury (SNI) rodent model of neuropathic pain. Western blot and immunohistochemistry studies revealed an increase in Slc7a5 protein levels in the spinal cord and DRGs of SNI mice compared to control mice. Using whole-cell current clamp electrophysiology, we observed that JPH203 treatment reduced excitability of small-diameter (<30 μm) DRG neurons from SNI mice, in agreement with its behavioral effects. Voltage-clamp recordings from JPH203-treated naïve rat DRGs identified an effect on tetrodotoxin-resistant (TTX-R) sodium currents. Altogether, these results demonstrate that Slc7a5 is dysregulated in chronic neuropathic pain and can be targeted to provide relief of hypersensitivity.

[†]corresponding authors: Sascha R.A. Alles salles@salud.unm.edu, Rajesh Khanna rkhanna@arizona.edu; rk4272@nyu.edu.

STATEMENTS AND DECLARATIONS

R. Khanna is the co-founder of Regulonix LLC, a company developing non-opioids drugs for chronic pain. In addition, R. Khanna 481 has patents US10287334 (Non-narcotic CRMP2 peptides targeting sodium channels for chronic 482 pain) and US10441586 (SUMOylation inhibitors and uses thereof) issued to Regulonix LLC. R. Khanna is also a co-founder of ElutheriaTx Inc., a company developing gene therapy approaches for chronic pain.

Keywords

Chronic Pain; Slc7a5 (LAT1); electrophysiology; nociceptor

INTRODUCTION

Slc7a5 (LAT1), also known as the system-L neutral amino acid transporter, is involved in many biological processes related to human health including cancer and inflammation [1]. Slc7a5 is expressed in nociceptors and the spinal dorsal horn. In our recent review [10, 21], we reported expression of Slc7a5 and its binding partner Slc3a2 in different transcriptionally defined dorsal root ganglia (DRG) subtypes as well as in both excitatory and inhibitory dorsal horn neurons in the spinal cord [1]. Slc7a5 is also expressed in neurons expressing other pain target genes of interest including *Scn9a* encoding the voltage-gated sodium channel $Na_v1.7$ implicated in congenital insensitivity to pain in humans [6].

Interestingly, Slc7a5 is best known as the transporter for the gabapentinoid drugs, gabapentin and pregabalin. These first-line, clinically available drugs for neuropathic pain are ligands of the α2δ-1 (alpha2delta-1) subunits of voltage-gated calcium channels, which is also upregulated in neuropathic pain states [14, 15]. Studies have demonstrated that Slc7a5 function is required for the gabapentinoid drugs to elicit their effects in reducing neuronal hyperexcitability in the spinal dorsal horn [4]. Slc7a5 has been shown to interact with key ion channels involved in pain including $Na_v1.7$ [11] and $K_v1.1/1.2$ [2, 12, 13]. Therefore, Slc7a5 is a novel target for the investigation of chronic pain mechanisms and possibly, development of therapeutics.

Here, we investigated the role of Slc7a5 in the spared nerve injury (SNI) model of neuropathic in rodents mainly using the Slc7a5 blocker, JPH203 [22]. We also compare the behavioral actions of Slc7a5 blockers and neuropathic pain state with cellular actions using electrophysiological methods.

MATERIALS AND METHODS

Spared Nerve Injury (SNI) model and Assessment of Behavior

The procedures in this study were approved by the Institutional Animal Care and Use Committees of the University of New Mexico and the University of Arizona. Male BALB/cAnNHsd mice (7–8 weeks old; Envigo Harlan) and Sprague Dawley rats (225–250 g; Envigo) were subjected to the spared nerve injury model of neuropathic pain as described previously[7]. Briefly, the tibial and common peroneal nerves were ligated and cut distal to the ligation site, but the sural nerve was spared. For sham surgeries, the nerve was exposed but not disturbed. The assessment of tactile allodynia was performed as reported previously using the “up and down” method [5]. All behavior and cell culture experiments with SNI rodents were conducted at 2–4 weeks post-injury.

DRG cultures

DRGs from all levels are isolated and acutely dissociated. Collected DRG is digested using dispase II and collagenase type 2. Cells are grown in DMEM medium (10% fetal bovine serum, 1% antibacterial/antimycotic) and incubated at 37°C, 5% CO_2 until use. Rat DRGs were prepared exactly as described [9, 16].

Current clamp recordings

Neurons are identified by infrared differential interference contrast (IR-DIC) connected to an Olympus digital camera. Current clamp recordings were performed using a Molecular Devices Multiclamp 700B (Scientifica, UK). Signals are filtered at 5 KHz, acquired at 50 KHz using a Molecular Devices 1550B converter (Scientifica, UK) and recorded using Clampex 11 software (Molecular Devices, Scientifica, UK). Electrodes were pulled with a Zeitz puller (Werner Zeitz, Martinsreid, Germany) from borosilicate thick glass (GC150F, Sutter Instruments). The resistance of the electrodes, following fire polishing of the tip, range between 5 and 8 MΩ. Bridge balance is applied to all recordings. Intracellular solution contains (in mM) 125 K-gluconate, 6 KCl, 10 HEPES, 0.1 EGTA, 2 Mg-ATP, pH 7.3 with KOH, and osmolarity of 290–310 mOsm. Artificial cerebrospinal fluid (aCSF) contains (in mM) 113 NaCl, 3 KCl, 25 NaHCO3, 1 NaH2PO4, 2 CaCl2, 2 MgCl2, and 11 D-glucose. DRG neurons were cultured from SNI mice at 2–4 weeks post-injury. Cultures were treated with either vehicle (0.1% DMSO) or JPH203 (10 μM) for 1 hr in vitro prior to electrophysiological recording and we recorded from small-diameter (<30 μm) DRG nociceptors.

Voltage clamp recordings

Patch-clamp recordings were performed at room temperature (22–24°C). Currents were recorded using an EPC 10 Amplifier-HEKA linked to a computer with Patchmaster software.

For total sodium current (I_{Na}) recordings, the external solution contained (in mM): 130 NaCl, 3 KCl, 30 tetraethylammonium chloride, 1 CaCl2, 0.5 CdCl2, 1 MgCl2, 10 D-glucose and 10 HEPES (pH 7.3 adjusted with NaOH, and mOsm/L= 324). Patch pipettes were filled with an internal solution containing (in mM): 140 CsF, 1.1Cs-EGTA, 10 NaCl, and 15 HEPES (pH 7.3 adjusted with CsOH, and mOsm/L= 311). Peak Na^+ current was acquired by applying 150-millisecond voltage steps from −70 to +60 mV in 5-mV increments from a holding potential of −60 mV to obtain the current-voltage (I-V) relation. Normalization of currents to each cell's capacitance (pF) was performed to allow for collection of current density data. For I-V adjustments, functions were fitted to data using a non-linear least squares analysis. I-V curves were fitted using double Boltzmann functions:

$$f = a + g1/(1 + exp((x - V_{1/2}1)/k1)) + g2/(1 + exp(-(x - V_{1/2}2)/k2))$$

where x is the prepulse potential, $V_{1/2}$ is the mid-point potential and k is the corresponding slope factor for single Boltzmann functions. Double Boltzmann fits were used to describe

the shape of the curve, not to imply the existence of separate channel populations. Numbers *1* and *2* simply indicate first and second mid-points; *a* along with *g* are fitting parameters.

Activation curves were obtained from the I-V curves by dividing the peak current at each depolarizing step by the driving force according to the equation: $G = I/(V_{mem}-E_{rev})$, where I is the peak current, V_{mem} is the membrane potential and E_{rev} is the reversal potential. The conductance (G) was normalized against the maximum conductance (Gmax). Steady-state inactivation (SSI) curves were obtained by applying an H-infinity protocol that consisted of 1-second conditioning pre-pulses from −120 to +10 mV in 10-mV increments followed by a 200-millisecond test pulse to +10 mV. Inactivation curves were obtained by dividing the peak current recorded at the test pulse by the maximum current (Imax). Activation and SSI curves were fitted with the Boltzmann equation.

Western blot and immunohistochemistry

Fresh DRG, spinal cord and brain tissue is homogenized, protein is isolated, separated by SDS-PAGE gel electrophoresis, and reacted with primary antibodies against monoclonal Anti-SLC7A5/LAT1 antibody (Abcam, ab208776) and the beta-actin loading control. Blots are washed, incubated with HRP conjugated secondary antibody and peroxidase activity detected by enhanced chemi-luminescence substrate reaction (ECL; Pierce). Quantifcation was performed using ImageJ.

For immunohistochemistry, cells were fixed in 2% paraformaldehyde and blocked in 2% FBS/BSA blocking buffer (1 hr) prior to overnight incubation in primary Anti-SLC7A5/LAT1 antibody (Abcam, ab208776). Images were collected by fluorescence microscopy.

Statistical and Data analysis

All statistical and data analysis was performed using GraphPad Prism 8. All data sets were checked for normality using D'Agostino & Pearson test. A p-value of less than 0.05 was considered statistically significant. Appropriate statistical tests performed are indicated in the text and figure legends.

RESULTS

Blocking Slc7a5 with JPH203 alleviates neuropathic pain

Since Slc7a5 is implicated in chronic pain [20], we used the Slc7a5 blocker JPH203 to determine whether blocking Slc7a5 could reverse mechanical allodynia in SNI rodents. We found that JPH203 (3 μg/ml) delivered by intrathecal injection significantly alleviated the hypersensitivity of male Sprague Dawley rats to a tactile stimulus with a peak anti-allodynic effect at approximately 3 hours post-injection (Figure 1, n=5 per group, $p<0.0001$, 2-way ANOVA). These results indicate that Slc7a5 is implicated in mechanical allodynia behaviors in rodents.

Spinal Slc7a5 protein levels are upregulated neuropathic pain

To determine if Slc7a5 is altered following development of mechanical allodynia in mice subjected to SNI, we examined protein levels of Slc7a5 in the spinal cord and DRG.

Whole spinal cord was obtained from SNI mice at peak pain behaviors. We demonstrate significant upregulation of Slc7a5 (Figure 2a–b, n=4 per condition, $p<0.05$ Mann-Whitney test) in the spinal cord of mice after SNI compared to naïve controls (Figure 2a–b). We performed further immunohistochemistry experiments on cultured DRG neurons from SNI and sham-injured mice and also noticed stark upregulation in DRGs from SNI compared to control cultures (Figure 2b). Therefore, Slc7a5 upregulation in the spinal cord may underlie its role in mechanical allodynia following nerve injury.

Slc7a5 blockade with JPH203 dampens nociceptor excitability from SNI mice

To further understand the mechanism of Slc7a5 in regulating neuropathic pain behaviors, we performed current clamp recordings of DRGs obtained from SNI mice. Our results show that rheobase of nociceptors was significantly increased (Figure 3a, $p<0.05$, Mann-Whitney test) following JPH203 treatment, while the resting membrane potential (RMP) was unchanged (Figure 3B). This indicates that JPH203 treatment reduces DRG excitability. We further studied excitability by applying depolarizing current ramps (Figure 3c). We noted a significant increase in the distribution of neurons under JPH203-treated conditions that fired 1 or no AP in response to ramp depolarization compared to controls (Figure 3d; $p<0.05$, Fisher's exact test). Again, these data confirm that JPH203-treatment reduced nociceptor excitability. We did not observe any differences in the number of APs fired or latency to the first spike fired for these ramp depolarization data (Figure 3e–f).

Slc7a5 blockade with JPH203 reduces nociceptor TTX-resistant Na^+ current peak amplitude

To elucidate the underlying mechanism of the effect of Slc7a5 blockade on nociceptor excitability, we performed voltage clamp recordings of Na^+ currents from nociceptors obtained from naïve rats in the presence and absence of JPH203 (10 μM). Our recordings did not reveal any differences in total Na^+ current density (Figure 4a–b), activation (Figure 4c) or inactivation (Figure 4d) kinetics in JPH203-treated DRGs compares to those treated with vehicle control. We found that JPH203 treatment significantly reduced the peak amplitude of TTX-R Na^+ current (Figure 4e; n=11–16 cells, $p<0.05$, t-test), but had no effect on TTX-S Na^+ current peak amplitude (Figure 4f). We also observed that the $V_{1/2}$ and slope factor of the activation and inactivation curves from the JP203-treated group is statistically different from that of the DMSO group ($p<0.01$, t-test, Table 1).

DISCUSSION

Our results provide evidence for a role of Slc7a5 in the pathogenesis of neuropathic pain. We demonstrate anti-allodynic actions of Slc7a5 blockade and corresponding upregulation of Slc7a5 in the SNI model. Previously, it has been shown that Slc7a5 protein levels are upregulated in the spinal cord in models of spinal cord injury [20]. Slc7a5 is best known as the transporter for the gabapentinoid drugs, gabapentin and pregabalin [4, 8]. These first-line, clinically available drugs for neuropathic pain are ligands of the α2δ-1 (alpha2delta-1) subunits of voltage-gated calcium channels, which are also upregulated in neuropathic pain states [14, 15].

Our immunohistochemistry data indicate differences in Slc7a5 staining in smaller versus larger diameter DRG neurons; however, more exhaustive studies of this are required. Our Western blot data of whole spinal cord indicates an increase in Slc7a5 under SNI conditions. The source of this increase within the cord is unknown. It is possible that there are differences in Slc7a5 expression across spinal laminae and/or levels both under baseline conditions, following different types of injury and at different time points following injury. In addition, the potential roles of glial cells with regards to Slc7a5's pronociceptive actions have yet to be investigated. Therefore, the cell-type specific upregulation of Slc7a5 after injury in the periphery, spinal cord and brain requires further study.

We show that Slc7a5 blockade dampens nociceptor excitability and that this effect may be due to an action on TTX-resistant Na^+ channels. While it has been shown that Slc7a5 does interact with the TTX-sensitive Na^+ channel Nav1.7, a clear functional relationship has not been demonstrated. We observed a leftward shift in the voltage dependence of inactivation in the presence of JPH203 of around −9 mV compared to the control group. This could be attributed to the effect of JPH203 on the TTX-R currents. Since TTX-R currents have slow and very slow inactivation kinetics [3], inhibiting these currents will shift the inactivation curve to more hyperpolarized potentials, which correlates with our findings. These findings indicate that further experiments are required to investigate the interactions between Slc7a5 and Na^+ channels.

These studies focus purely on the neuronal mechanisms of Slc7a5 in neuropathic pain, but more work is required to study its non-neuronal mechanisms as well since Slc7a5 is also involved in amino acid transport and regulating the function of immune cells such as T-cells [17, 18] and B-cells [19].

Future work will involve the use of knockout mice and further mechanistic studies will aid in the development of Slc7a5 inhibitors that are optimal for reversing the pathophysiology of chronic pain. Long-term studies of the effect of Slc7a5 inhibitors such as cytokine profiling and RNA-seq on isolated tissues from treated animals will also be necessary to understand the role of Slc7a5 in chronic pain. In summary, these results demonstrate that Slc7a5 is dysregulated in chronic neuropathic pain and can be targeted to provide relief of hypersensitivity.

ACKNOWLEDGEMENTS

We thank Prof. Karin N. Westlund and Dr. Sabrina McIlwrath for assistance with immunohistochemistry experiments. We thank Marena Montera for assistance with Western blot experiments and lab management.

Funding:

S.R.A.A acknowledges funding from the Research Endowment Fund of the Department of Anesthesiology and Critical Care Medicine, University of New Mexico School of Medicine. Supported by National Institutes of Health awards (NINDS (NS098772 and NS120663 to RK).

REFERENCES

1. Alles SRA, Gomez K, Moutal A, Khanna R (2020) Putative roles of SLC7A5 (LAT1) transporter in pain. Neurobiol Pain 8:100050. doi: 10.1016/j.ynpai.2020.100050 [PubMed: 32715162]

2. Baronas VA, Yang RY, Morales LC, Sipione S, Kurata HT (2018) Slc7a5 regulates Kv1.2 channels and modifies functional outcomes of epilepsy-linked channel mutations. Nat Commun 9:4417. doi: 10.1038/s41467-018-06859-x [PubMed: 30356053]

3. Bennett DL, Clark AJ, Huang J, Waxman SG, Dib-Hajj SD (2019) The Role of Voltage-Gated Sodium Channels in Pain Signaling. Physiol Rev 99:1079–1151. doi: 10.1152/physrev.00052.2017 [PubMed: 30672368]

4. Biggs JE, Boakye PA, Ganesan N, Stemkowski PL, Garcia AL, Ballanyi K, Smith PA (2014) Analysis of the Long-Term Actions of Gabapentin and Pregabalin in Dorsal Root Ganglia and Substantia Gelatinosa. J Neurophysiol. doi: 10.1152/jn.00168.2014

5. Chaplan SR, Bach FW, Pogrel JW, Chung JM, Yaksh TL (1994) Quantitative assessment of tactile allodynia in the rat paw. J Neurosci Methods 53:55–63. doi: 10.1016/0165-0270(94)90144-9 [PubMed: 7990513]

6. Cox JJ, Reimann F, Nicholas AK, Thornton G, Roberts E, Springell K, Karbani G, Jafri H, Mannan J, Raashid Y, Al-Gazali L, Hamamy H, Valente EM, Gorman S, Williams R, McHale DP, Wood JN, Gribble FM, Woods CG (2006) An SCN9A channelopathy causes congenital inability to experience pain. Nature 444:894–898. doi: 10.1038/nature05413 [PubMed: 17167479]

7. Decosterd I, Woolf CJ (2000) Spared nerve injury: an animal model of persistent peripheral neuropathic pain. Pain 87:149–58 [PubMed: 10924808]

8. Dickens D, Webb SD, Antonyuk S, Giannoudis A, Owen A, Rädisch S, Hasnain SS, Pirmohamed M (2013) Transport of gabapentin by LAT1 (SLC7A5). Biochem Pharmacol 85:1672–1683. doi: 10.1016/j.bcp.2013.03.022 [PubMed: 23567998]

9. François-Moutal L, Wang Y, Moutal A, Cottier KE, Melemedjian OK, Yang X, Wang Y, Ju W, Largent-Milnes TM, Khanna M, Vanderah TW, Khanna R (2015) A membrane-delimited N-myristoylated CRMP2 peptide aptamer inhibits CaV2.2 trafficking and reverses inflammatory and postoperative pain behaviors. Pain 156:1247–1264. doi: 10.1097/j.pain.0000000000000147 [PubMed: 25782368]

10. Häring M, Zeisel A, Hochgerner H, Rinwa P, Jakobsson JET, Lönnerberg P, Manno G, Sharma N, Borgius L, Kiehn O, Lagerström MC, Linnarsson S, Ernfors P (2018) Neuronal atlas of the dorsal horn defines its architecture and links sensory input to transcriptional cell types. Nat Neurosci 1. doi: 10.1038/s41593-018-0141-1

11. Kanellopoulos AH, Koenig J, Huang H, Pyrski M, Millet Q, Lolignier S, Morohashi T, Gossage SJ, Jay M, Linley JE, Baskozos G, Kessler BM, Cox JJ, Dolphin AC, Zufall F, Wood JN, Zhao J (2018) Mapping protein interactions of sodium channel NaV1.7 using epitope-tagged gene-targeted mice. EMBO J e96692. doi: 10.15252/embj.201796692

12. Lamothe SM, Kurata HT (2020) Slc7a5 alters Kvβ-mediated regulation of Kv1.2. J Gen Physiol 152. doi: 10.1085/jgp.201912524

13. Lamothe SM, Sharmin N, Silver G, Satou M, Hao Y, Tateno T, Baronas VA, Kurata HT (2020) Control of Slc7a5 sensitivity by the voltage-sensing domain of Kv1 channels. eLife 9:e54916. doi: 10.7554/eLife.54916 [PubMed: 33164746]

14. Luo ZD, Calcutt NA, Higuera ES, Valder CR, Song YH, Svensson CI, Myers RR (2002) Injury type-specific calcium channel alpha 2 delta-1 subunit up-regulation in rat neuropathic pain models correlates with antiallodynic effects of gabapentin. J Pharmacol Exp Ther 303:1199–205. doi: 10.1124/jpet.102.041574 [PubMed: 12438544]

15. Luo ZD, Chaplan SR, Higuera ES, Sorkin LS, Stauderman KA, Williams ME, Yaksh TL (2001) Upregulation of dorsal root ganglion (alpha)2(delta) calcium channel subunit and its correlation with allodynia in spinal nerve-injured rats. J Neurosci 21:1868–75 [PubMed: 11245671]

16. Moutal A, Chew LA, Yang X, Wang Y, Yeon SK, Telemi E, Meroueh S, Park KD, Shrinivasan R, Gilbraith KB, Qu C, Xie JY, Patwardhan A, Vanderah TW, Khanna M, Porreca F, Khanna R (2016) (S)-lacosamide inhibition of CRMP2 phosphorylation reduces postoperative and neuropathic pain behaviors through distinct classes of sensory neurons identified by constellation pharmacology. Pain 157:1448–1463. doi: 10.1097/j.pain.0000000000000555 [PubMed: 26967696]

17. Powell JD (2013) Slc7a5 helps T cells get with the program. Nat Immunol 14:422–424. doi: 10.1038/ni.2594 [PubMed: 23598390]

18. Sinclair LV, Rolf J, Emslie E, Shi Y-B, Taylor PM, Cantrell DA (2013) Control of amino-acid transport by antigen receptors coordinates the metabolic reprogramming essential for T cell differentiation. Nat Immunol 14:500–508. doi: 10.1038/ni.2556 [PubMed: 23525088]

19. Torigoe M, Maeshima K, Ozaki T, Omura Y, Gotoh K, Tanaka Y, Ishii K, Shibata H (2019) l-Leucine influx through Slc7a5 regulates inflammatory responses of human B cells via mammalian target of rapamycin complex 1 signaling. Mod Rheumatol 29:885–891. doi: 10.1080/14397595.2018.1510822 [PubMed: 30092695]

20. Toyooka T, Nawashiro H, Shinomiya N, Yano A, Ooigawa H, Ohsumi A, Uozumi Y, Yanagawa Y, Matsuo H, Shima K (2008) Up-regulation of L type amino acid transporter 1 after spinal cord injury in rats. Acta Neurochir Suppl 102:385–388. doi: 10.1007/978-3-211-85578-2_74 [PubMed: 19388351]

21. Usoskin D, Furlan A, Islam S, Abdo H, Lönnerberg P, Lou D, Hjerling-Leffler J, Haeggström J, Kharchenko O, Kharchenko PV, Linnarsson S, Ernfors P (2014) Unbiased classification of sensory neuron types by large-scale single-cell RNA sequencing. Nat Neurosci 18:145–153. doi: 10.1038/nn.3881 [PubMed: 25420068]

22. Wempe MF, Rice PJ, Lightner JW, Jutabha P, Hayashi M, Anzai N, Wakui S, Kusuhara H, Sugiyama Y, Endou H (2012) Metabolism and pharmacokinetic studies of JPH203, an L-amino acid transporter 1 (LAT1) selective compound. Drug Metab Pharmacokinet 27:155–161 [PubMed: 21914964]

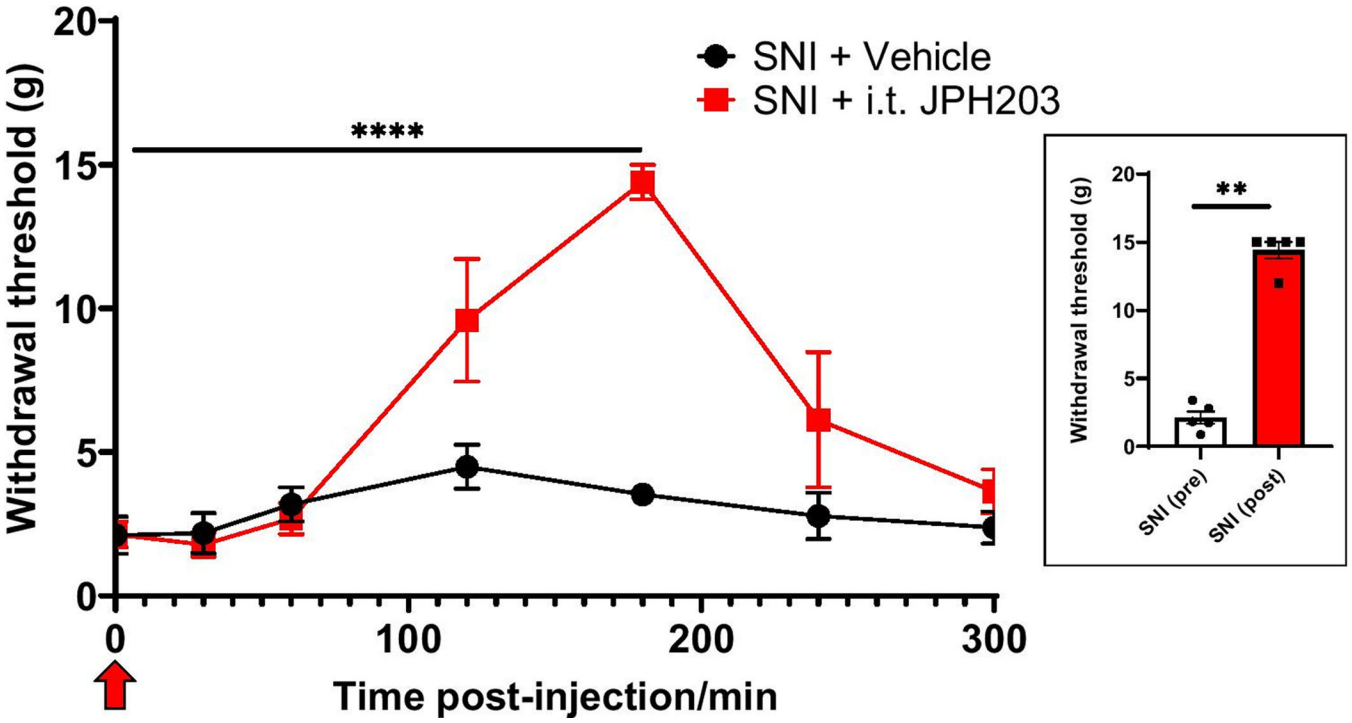

Figure 1. Blockade of Slc7a5 with JPH203 alleviates neuropathic pain in the SNI rodent model.

Alleviation of neuropathic pain in rats (two weeks after SNI) following intrathecal injection (n=5 per group, ****p<0.0001, 2-way ANOVA) of the Slc7a5 blocker, JPH203. At peak anti-allodynic effect at 180 min post-injection, paw withdrawal threshold values were Control: 3.53 ± 0.344 g and JPH203: 14.4 ± 0.65 g. Inset indicates the area under the curve (AUC) derived using GraphPad Prism. Red arrow indicates time of JPH203 injection. Experimenter was blinded to the treatment condition.

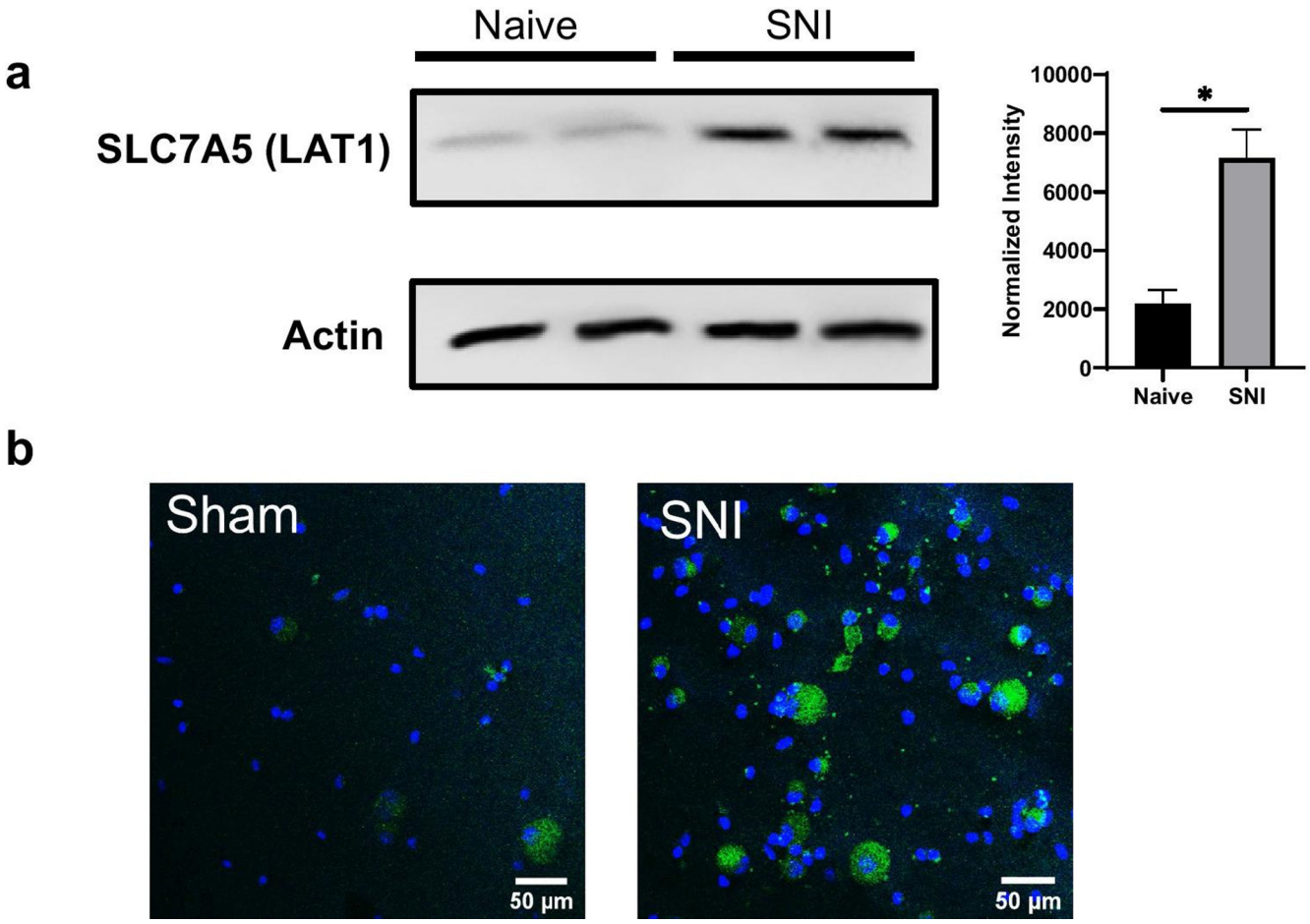

Figure 2. Upregulation of Slc7a5 (Lat1) in spinal cord and DRGs of SNI mice.

a. Western blot showing an increase in Slc7a5 protein levels in the spinal cord of SNI mice compared to naïve mice Inset: normalized intensity (Naïve: 2188 ± 234 a.u., SNI: 7159 ± 485 a.u., n=4 per condition, $p<0.05$, *Mann-Whitney test) **b.** Confocal images of immunohistochemical staining for Slc7a5 (green) in DRG cultures from SNI mice. DAPI staining is shown in blue.

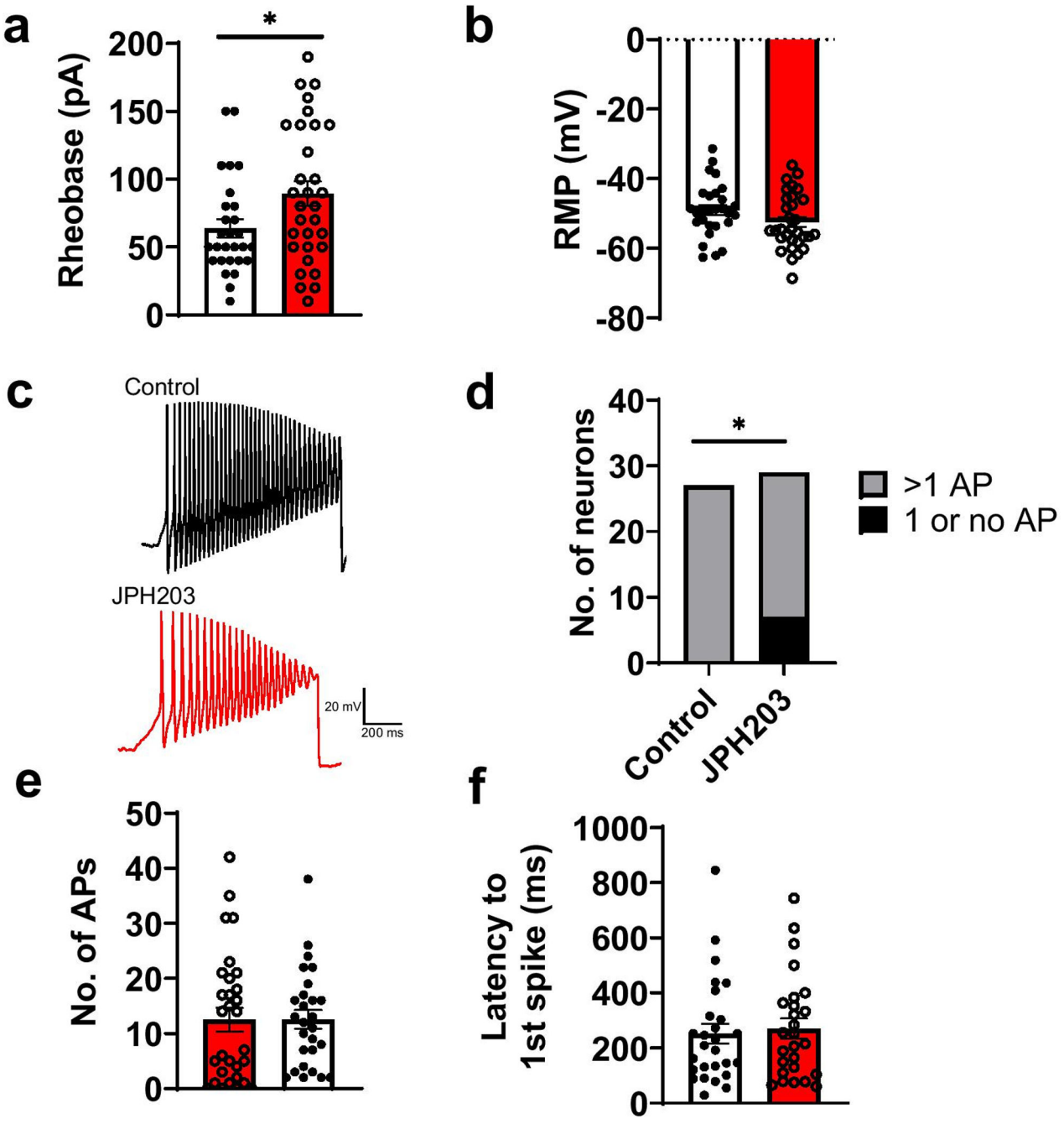

Figure 3. Effect of Slc7a5 blockade with JPH203 (10 μM) on small-diameter (<30 μm) DRG neuron excitability from SNI mice.

a. Rheobase (current required to elicit firing) was significantly increased (Control: 63.9 ± 6.67 pA, JPH203: 89.4 ± 9.09 pA, *p<0.05, Mann-Whitney test), but **b.** resting membrane potential (RMP) was not significantly changed in the presence of JPH203 (Control: −49.0 ± 1.45 mV, JPH203: −52.4 ± 1.43 mV, p>0.05, Mann-Whitney test) (n= 28 vehicle, n=31 JPH203-treated neurons). **c.** Representative current clamp recordings from SNI DRG neurons in response to depolarizing current ramps (500 pA/s) Current ramp recordings show that the **d.** distribution of neurons was significantly different (*p<0.05, Fisher's exact

test) in the JPH203-treated group compared to controls (n=27 vehicle, n=30 JPH203-treated neurons), but the **e.** no. of Aps (Control: 12.6 ± 1.71, JPH203: 12.5 ± 2.15, p>0.05, Mann-Whitney test) and **f.** latency to 1st spike (Control: 252 ± 36.1, JPH203: 271 ± 36.5, p>0.05, Mann-Whitney test) were not significantly different in the presence of JPH203 compared to controls.

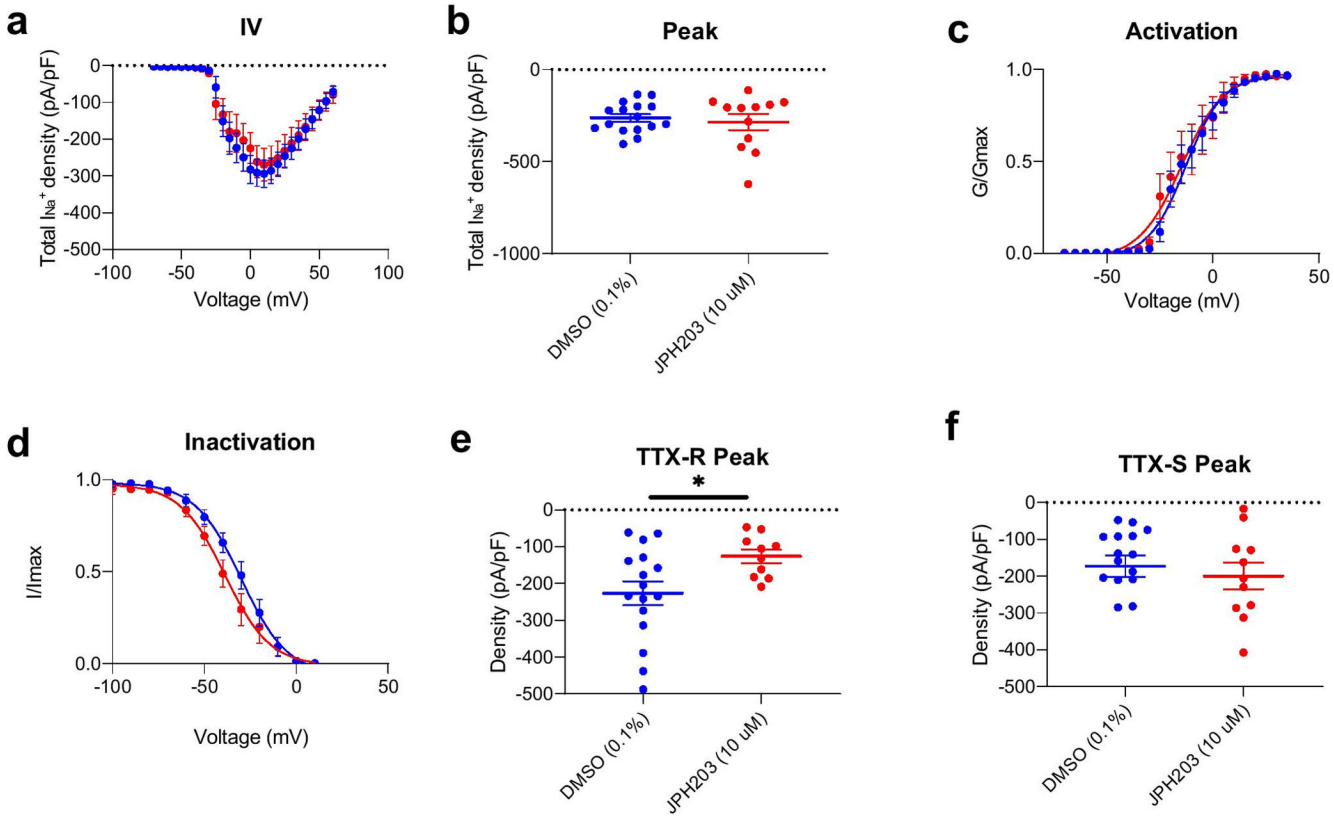

Figure 4. Effect of Slc7a5 blockade on Na+ currents recorded from rat DRG neurons.

a. Total Na^+ current density. **b.** Peak I_{Na} (Control: −262 ± 20.4 mV, JPH203: −285 ± 43.3 mV) **c.** Activation and **d.** Inactivation plots for I_{Na}. **e.** TTX-resistant (TTX-R) peak (Control: −227 ± 32.2 mV, JPH203: −126 ± 18.1 mV), but not **f**. TTX-sensitive (TTX-S) Na^+ current peak (Control: −173 ± 28.8 mV, JPH203: −200 ± 35.8 mV) was significantly reduced following JPH203 treatment (n=11–16 cells, *p<0.05, Student's t-test). Results of activation and inactivation curve fitting are shown in Table 1.

Table 1.

Gating properties of sodium currents recorded from rat DRG neurons.

	DMSO (0.1%)	JPH203 (10 μM)
Activation		
$V_{1/2}$	−12.925 ± 1.095 (17)	−14.832 ± 1.778 (11)
k	8.648 ± 0.999 (17)	10.015 ± 1.676 (11)
Inactivation		
$V_{1/2}$	−29.851 ± 1.941 (16)	−38.745 ± 2.147 (11)*
k	−12.605 ± 1.768 (16)	−12.263 ± 2.076 (11)

Values are means ± SEM calculated from fits of the data from the indicated number of individual cells (in parentheses) to the Boltzmann equation; $V_{1/2}$ mid-point potential (mV) for voltage-dependent of activation or inactivation; k, slope factor. These values pertain to Fig. 4c and 4d.

*Indicate statistical difference compared to the DMSO group (p= 0.0057). Data were analyzed with unpaired t test.